Quaternary International 536 (2020) 75–84

Contents lists available at ScienceDirect

Quaternary International

journal homepage: www.elsevier.com/locate/quaint

Climatic and human impact on the environment: Insight from the tetraether lipid temperature reconstruction in the Beibu Gulf, China

Weisen Liao[a,b], Jianfang Hu[a,c,*], Haoda Zhou[a,d], Ping'an Peng[a,b]

[a] State Key Laboratory of Organic Geochemistry, Guangzhou Institute of Geochemistry, Chinese Academy of Sciences Guangzhou, 510640, China
[b] University of Chinese Academy of Sciences, Beijing, 100049, China
[c] Key Laboratory of Ocean and Marginal Sea Geology, Chinese Academy of Sciences, Guangzhou, 510640, China
[d] Laboratory of Marine Ecosystem and Biogeochemistry, Second Institute of Oceanography, SOA, Hangzhou, 310012, China

ARTICLE INFO

Keywords:
GDGTs
BIT
Temperature reconstruction
Anthropogenic influences
East Asian monsoon

ABSTRACT

Organic proxies have been widely used to reconstruct temperature and terrestrial input variation at the interface between land and sea. However, the impact of human activities on these proxies has been little constrained, which might cause the misinterpretation of the sediment profile. In order to study the climatic and human impact on the environment, proxies in coastal regions, glycerol dialkyl glycerol tetraethers (GDGTs) in a sediment core spanning 115 years was analyzed from Beibu Gulf, China. The results indicate that isoprenoid GDGTs in the Beibu Gulf were mainly derived from Thaumarchaeota and the branched GDGTs originated mainly from terrestrial soil bacteria. The TEX_{86} index was applied to reconstruct the temporal SST variation. The results show that variation of TEX_{86}-derived SST is controlled mainly by East Asian Monsoon system and partly by ENSO events. The methylation index of branched tetraethers or the cyclization index of branched tetraethers (MBT/CBT) derived mean annual air temperature (MAAT) agreed with MAAT record at the Qinzhou Station before 1982 AD. However, the population growth and economic development after 1982 AD caused the reduction of terrestrial organic matter input and increase of nutrient, leading to the thriving of Thaumarchaeota and increasing of *in situ* branched GDGTs proportion, which created the scatter of the MBT/CBT-reconstructed MAAT after 1982 AD. Therefore, human influence on GDGT proxies can be constrained in this way to avoid misinterpretation of paleoclimate and paleoenvironment records.

1. Introduction

The global climate is characterized with unprecedented temperature rise since the late 19th century as suggested by numerous instrumental records and the Intergovernmental Panel on Climate Change (IPCC) Assessment Report (IPCC, 2013). However, the instrumental records are too short to comprehensively assess anthropogenic impacts on the climate change, especially in the tropical area (Abram et al., 2016). Beyond the instrumental record, the reconstruction of natural climate variability based on reliable proxies replenishes a better understanding of the climate system at longer timescales and a trustworthy prediction of climate change scenarios (Jansen et al., 2007). Organic matter (OM) constitutes a minor fraction of marine and freshwater sediments, yet its important contribution to the sedimentary record can be used to reconstruct the marine and continental paleoenvironment (Meyers, 1997). Numerous organic proxies have been used to reconstruct paleoclimate and paleoenvironment (Eglinton and Eglinton, 2008).

Coastal seas and estuaries are sites of significant land–sea interaction, and compared with their surface area, these transitional regions along the continental margins play a disproportionately important role in the biogeochemical cycles. Moreover, since 75% of the world's population is located in the coastal regions (Canuel et al., 2012), the anthropogenic impacts on environment might be as important as the natural climatic impacts. Human impacts on the coastal environment include altered river discharge and salinity due to water management projects such as dams; and conversion of land to agriculture, grazing, and urban uses (Lotze, 2010). The resultant environmental consequences (e.g., increased phytoplankton production, oxygen deficiency, and decreased biodiversity) may alter the composition of OM deposited in the coastal and marine regions (Cloern, 2001; Diaz and Rosenberg, 2008). Like other major estuarine systems worldwide, the Beibu Gulf has been increasingly impacted by human activities. Over the past decade, rapid industrialization and urbanization have led to increasing stresses on the ecosystem structure and environmental

* Corresponding author. Guangzhou Institute of Geochemistry, Chinese Academy of Sciences Guangzhou, GD, 510640, PR China.
E-mail address: hujf@gig.ac.cn (J. Hu).

https://doi.org/10.1016/j.quaint.2019.12.004
Received 6 May 2019; Received in revised form 28 September 2019; Accepted 3 December 2019
Available online 09 December 2019
1040-6182/

quality (Xia et al., 2011; Zhang et al., 2014; Zheng et al., 2012). For example, eutrophication or even seasonal hypoxia has occurred in the Qinzhou Bay, located in the northern Beibu Gulf (Lai et al., 2014). As one of the major aquaculture areas of China and Vietnam, the Beibu Gulf receives a massive flux of anthropogenic nutrients from fish farming. Meanwhile, the nutrients from agricultural activities and sewage are transported to the estuarine system. As a result, the phytoplankton productivity is highly variable across the gulf. These changes may potentially alter the nature and OM content in the marine sediments (Owen and Lee, 2004).

Glycerol dialkyl glycerol tetraethers (GDGTs) are membrane lipids produced by archaea and bacteria (Schouten et al., 2013; Sinninghe Damsté et al., 2000; Weijers et al., 2006a). They are generally divided into isoprenoid and branched groups. The isoprenoid GDGTs (isoGDGTs) are produced by at least two groups of Archaea, Thaumarchaeota (formerly marine group I Crenarchaeota) and Euryarchaeota and occur mostly in the form of acyclic or ring containing biphytanyl chains (De Rosa and Gambacorta, 1988; Koga and Morii, 2007). The TEX_{86} proxy was proposed for the estimation of past sea surface temperature (SST) by Schouten et al. (2002), which has been successfully applied to the reconstruction of paleotemperatures in the oceans and large lakes (e.g. Powers et al., 2004, 2010).

Branched GDGTs (brGDGTs) with variable numbers of branching methyl groups (4–6) and containing up to two cyclopentane moieties were initially thought to be derived from terrestrial soils (Sinninghe Damsté et al., 2000; Weijers et al., 2006b) and subsequently transported and deposited in near-coastal marine sediments (Peterse et al., 2009), although they could be produced by anaerobic and heterotrophic bacteria in aquatic environments (Schouten et al., 2013; Zell et al., 2014; Zhou et al., 2014). Recently, Sinninghe Damsté (2016) proposed the $\#rings_{tetra}$ value to distinguish soil-derived brGDGTs and *in situ* produced brGDGTs in aquatic environments. Weijers et al. (2007b) demonstrated that the relative distribution of the brGDGTs in soil is controlled primarily by the air temperature and soil pH. The CBT (cyclization ratio of branched tetraethers) is related to soil pH and the MBT (methylation index of branched tetraethers) is a function of both soil pH and mean annual air temperature (MAAT; Weijers et al., 2007b), which have been widely used to the reconstruction of paleoenvironment in coastal areas (Weijers et al., 2007a; Ge et al., 2014; Chen et al., 2018). Another index, the Branched Isoprenoid Tetraether (BIT) was proposed to calculate the relative abundance of terrestrial soil OM in aquatic environments (Hopmans et al., 2004).

Previous studies have shown that the organic proxy sedimentary records are influenced not only by the climate but also by human activities (Chen et al., 2017, 2018; Lammers et al., 2013; Meng et al., 2016; Wu et al., 2013). However, due to the increasing anthropogenic influences on the coastal environment, more detailed information on the anthropogenic influences is still needed. In this study, we reconstruct the climatic/environmental changes based on the GDGT-based proxies in the core sediments from the Beibu Gulf, China, with the aim to better understand the variations of TEX_{86}-derived SSTs, CBT/MBT-derived MAATs, and CBT-derived pH in response to natural and anthropogenic affected climatic and environmental changes.

2. Materials and methods

2.1. Study area and sampling

The Beibu Gulf, located in the northwest South China Sea (SCS), spans the Guangdong coast from Hainan Island to the border with Guangxi (Ma et al., 2010), covering an area of approximately 128,000 km^2 (Fig. 1). The water depth in the Beibu Gulf is typically less than 100 m, with a mean depth of 50 m, and the annual SST are around 23.9 °C (Chen et al., 1998). The climate is subtropical and monsoonal (Chen et al., 2009). Monthly average air temperature ranges from 13.4 °C to 28.3 °C, with an average of 22.4 °C. Average annual rainfall is ~2100 mm, with 80–85% of rainfall occurring during the summer. The Beibu Gulf is fed by numerous tributary estuaries, where rivers discharge nutrients into the gulf (Zheng et al., 2012).

Sediment core SN2 (Fig. 1) was collected from the Beibu Gulf (21°35.1130′N, 108°45.4790′E) in December 2010. A stainless steel static gravity corer (8 cm i.d.) was employed to minimize the disturbance of surface sediment layers. The core samples were sliced at 1 cm intervals to the depth of 50 cm aboard ship. The sliced sediment samples were sealed in polyethylene bags and stored at −20 °C until analysis.

2.2. Sediment core dating

The age model of core SN2 was established using ^{210}Pb dating of 14 core sediment samples. In brief, the ^{210}Pb activities in sediment subsamples were determined by analysis of α-radioactivity of its decay product ^{210}Po, with the assumption that these two were in equilibrium. The Po was extracted, purified, and self-plated onto silver disks at 75–80 °C in 0.5 M HCl, with ^{209}Po used as a yield monitor and tracer in quantification. Counting was conducted by computerized multichannel α-spectrometry with gold–silicon surface barrier detectors. Supported ^{210}Po was obtained by indirectly determining the α-activity of the supporting parent ^{226}Ra, which was carried by co-precipitated $BaSO_4$.

2.3. Analysis of GDGTs

A total of 10–15 g of each powdered sample was spiked with an appropriate amount of C_{46}-GDGT standard compound, then extracted via Soxhlet reflux for 48 h using a mixture of dichloromethane (DCM) and methanol (2:1, V/V). The resulting mixture was centrifuged, and the organic phase was separated from the aqueous phase using a separation funnel following an addition of 5% KCl solution. The aqueous phase was extracted with DCM (× 3), and the collected organic material was concentrated by rotary evaporation. The total lipid extract was fractionated by column chromatography using neutral alumina. The non-polar and polar fractions were eluted with a hexane/DCM mixture (9:1, v:v) and a DCM/methanol methanol (1:1, v:v), respectively. The polar fraction (DCM/methanol) was dried under a stream of N_2, redissolved in a hexane/isopropanol mixture (99:1, v/v), and filtered through a 0.45 μm polytetrafluoroethene filter prior to analysis.

High-performance liquid chromatography/atmospheric pressure chemical ionization-mass spectrometry (HPLC/APCI-MS) was used to analyze the GDGT content of all samples. Analyses were performed using an Agilent 1200 series liquid chromatograph, equipped with autoinjector and ChemStation chromatography management software. The specific parameters of the HPLC/APCI-MS analysis followed those described in Zhou et al. (2014). GDGTs were detected using selected ion monitoring (SIM) mode, following the methods described in Schouten et al. (2007). Integration of the peak area of $[M+H]^+$ ion traces was used to quantify GDGT content. Each sample was analyzed in duplicate, and the data presented are mean values.

Proxies based on the distribution of GDGTs were calculated as following:

$$BIT = \frac{Ia + IIa + IIIa}{(Ia + IIa + IIIa + Cren.)}$$ (Hopmans et al., 2004);

MBT = (Ia + Ib + Ic) / (Ia + Ib + Ic + IIa + IIb + IIc + IIIa + IIIb + IIIc) (Weijers et al., 2007b);

MBT' = (Ia + Ib + Ic) / (Ia + Ib + Ic + IIa + IIb + IIc + IIIa) (Peterse et al., 2012);

CBT = - log ((Ib + IIb) / (Ia + IIa)] (Weijers et al., 2007b);

$\#rings_{tetra}$ = (Ib + 2*Ic) / (Ia + Ib + Ic) (Sinninghe Damsté, 2016);

MI = (GDGT-1 + GDGT-2 + GDGT-3) / (GDGT-1 + GDGT-2 + GDGT-

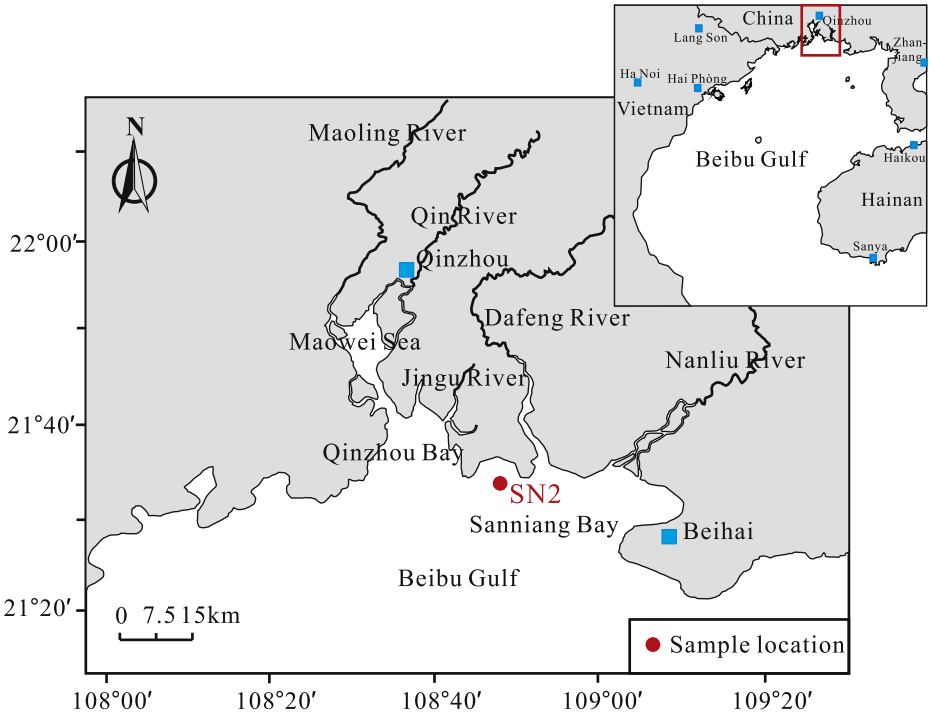

Fig. 1. The location of sediment core SN2 in the Beibu Gulf, China. The location of the Beibu Gulf is shown in the inserted map. Rivers and cities in the adjacent regions are shown.

3 + Cren + Cren') (Zhang et al., 2011);

TEX_{86} = (GDGT-2 + GDGT-3 + Cren') / (GDGT-1 + GDGT-2 + GDGT-3 + Cren') (Schouten et al., 2002);

where Ia–IIIc refer to branched GDGTs with various degrees of cyclization and branches as shown in Fig. S1.

TEX_{86}^{H} has been suggested by Kim et al. (2010) as an index of annual SST in tropical/subtropical oceans, where SSTs are > 15 °C, as follows:

$$TEX_{86}^{H} = (GDGT{-}2 + GDGT - 3 + Cren') / (GDGT{-}1 + GDGT - 2 + GDGT - 3 + Cren')$$

$$SST = 68.4 \times TEX_{86}^{H} + 38.6 (R^2 = 0.87 \ , n = 255)$$

We used the MAT and pH calibrations of Weijers et al. (2007b) based on global datasets which are calculated as below:

$$MBT = 0.122 + 0.187 \times CBT + 0.020 \times MAT \ (R^2 = 0.77, n = 114);$$

$$CBT = 3.33–0.38 \times pH \ (R^2 = 0.70, n = 114)$$

3. Results

3.1. Radionuclide activity profiles and geochronology

The $^{210}Pb_{tot}$ for SN2 ranged from 1.28 to 4.17 dpm/g and ^{226}Ra ranged from 0.60 to 0.23 dpm/g. The $^{210}Pb_{ex}$ activity curve in the core is shown in Fig. 2a. Presence of $^{210}Pb_{ex}$ was noted until 50 cm. The ^{210}Pb activity after 30 cm was constant and hence, it was assumed to represent supported activity. $^{210}Pb_{ex}$ declined from the maximum value of 3.43 dpm/g near the surface to 1.03 at 25 cm depth. $^{210}Pb_{ex}$ exhibited a monotonically decreasing trend (Fig. 2a). The natural logarithm of $^{210}Pb_{ex}$, ln ($^{210}Pb_{ex}$) was linearly correlated with depth (correlation coefficient R^2 = 0.75; Fig. 2a). The CRS (Constant Rate of Supply) method of ^{210}Pb dating was used to calculate the sedimentation rate. The model assumed a constant ^{210}Pb flux, but variable

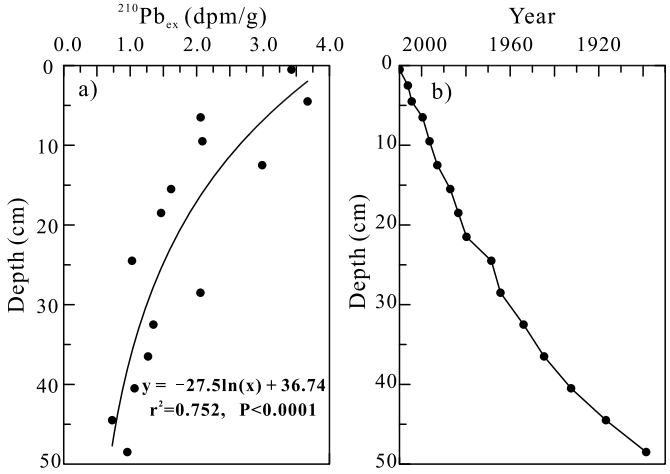

Fig. 2. Vertical distributions of (a) $^{210}Pb_{ex}$, (b) sedimentation rate (SR), and (c) ^{210}Pb chronology from SN2.

sedimentation rate. Average sedimentation rate based on the CRS method was estimated as 4.3 mm/yr. Based on these, the deepest part of the core was dated to be ~AD 1894 (Fig. 2b).

3.2. GDGT abundances and compositions

Isoprenoid and branched GDGTs were detected in the whole core sediments. The concentrations of isoGDGTs range from 0.06 to 6.43 ng g^{-1} dry weight (dw) (Fig. 3b). The isoGDGTs are dominated by crenarchaeol (cren.) and GDGT-0, accounting for 21.0–29.5% and 47.3–61.1% of total isoGDGTs, respectively. The compositional distribution of isoGDGTs remains relatively stable throughout the core.

The concentrations of branched GDGTs in the core sediment range from 0.04 to 7.00 ng g^{-1} dry weight, accounting for 13.0–58.1% of total GDGTs (Fig. 3a). The brGDGTs are dominated by GDGT-I compounds (i.e., GDGT-Ia, Ib, and Ic, accounting for 63.9–73.8% of

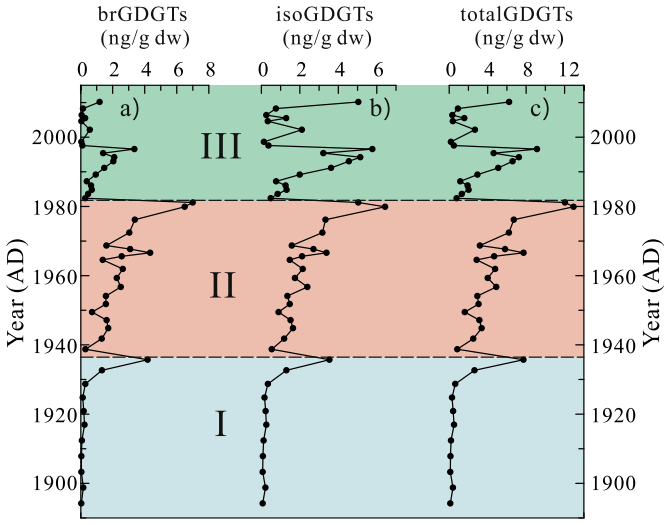

Fig. 3. Temporal variations of concentration of a) brGDGTs, b) isoGDGTs and c) total GDGTs.

branched GDGTs) and GDGT-II (accounting for 20.1–30.5% of branched GDGTs). The percentage of total branched GDGTs is relatively high during 1936–1982 (Fig. 3).

The concentrations of total GDGTs range from 0.11 to 12.93 ng g^{-1} dw (Fig. 3c), and is relatively low from 1894 to 1936 (average 1.19 ng g^{-1} dw), increasing from 1936 to 1982 (average 4.91 ng g^{-1} dw) and moderate from 1982 to 2010 (average 2.92 ng g^{-1} dw). According to the temporal distribution of the GDGTs, Core SN2 could be divided into three sections: 40–50 cm (section I), 20–40 cm (section II) and 0–20 cm (section III), which represents 1894–1936 AD, 1936–1982 AD and 1982–2010 AD, respectively (Fig. 3). Section I is characterized by low GDGT concentrations with low concentration of brGDGTs and isoGDGTs. Section II is characterized by high GDGT concentrations with increasing concentrations of both brGDGTs and isoGDGTs. Meanwhile, Section III is characterized by low brGDGTs concentrations and relatively high isoGDGTs concentrations (Fig. 3).

3.3. GDGT-0/cren, MI, BIT, #rings$_{tetra}$, TEX$_{86}$, MBT, and CBT values

The GDGT-0/Cren ratio ranges from 0.34 to 0.62 and decreases slowly upward (Fig. 4a). The Methane Index (MI) ratio ranges from 0.21 to 0.35 and displays a similar trend with GDGT-0/Cren ratio (Fig. 4b). The #rings$_{tetra}$ values vary between 0.46 and 0.32 (Fig. 4c). The BIT indices range from 0.16 to 0.66 in the full set of samples (Fig. 4d). While TEX_{86}^{H} values ranges from -0.45 to -0.24. The MBT ratios vary between 0.64 and 0.74 in core SN2, while CBT values range from 0.52 to 0.74.

From 1894 to 1936 AD, the BIT indices are relatively high and the TEX_{86}^{H} values are relatively low. Then the BIT indices and the TEX_{86}^{H} values increase to the highest from 1936 AD to 1982 AD. The period of 1982 AD to 2010 AD is characterized by decreasing BIT index and TEX_{86}^{H} values. For the three sections the average BIT index is 0.56, 0.60 and 0.33, and the average TEX_{86}^{H} is -0.39, -0.28 and -0.32 from bottom to surface, respectively.

3.4. TEX_{86}^{H}-derived temperatures, MBT/CBT-derived MAAT, and CBT-derived pH

The TEX_{86}^{H}-derived SST are between 7.9 and 22.2 °C (Fig. 5a) and the MBT/CBT-derived MAAT range from 19.2 to 25.0 °C (Fig. 6a), while the MBT'/CBT-derived MAAT range from 16.6 to 22.2 °C. The CBT-derived pH values vary between 6.5 and 6.9 (Fig. 4e). The TEX_{86}^{H}-derived SST increase from 1894–1936 AD (average 12.1 °C) to 1936–1982 AD (average 19.3 °C) and decrease toward 1982–2010 AD (average 16.8 °C). The MAAT values are relatively stable, decrease from 1894–1936 AD (average 22.4 °C) to the 1936–1982 AD (average 21.8 °C) and increase slightly towards 1982–2010 AD (average 22.0 °C).

4. Discussion

4.1. Sources of GDGTs

4.1.1. IsoGDGTs

The isoGDGTs were dominated by crenarchaeol and GDGT-0 in Core SN2. Although crenarchaeol is only produced by Thaumarchaeota (de la Torre et al., 2008; Hopmans et al., 2004; Pearson et al., 2004), GDGT-0, as well as GDGT-1, 2, 3, may be produced by many archaea, including Thaumarchaeota and methanogenic Euryarchaeota (Pancost et al., 2001). However, methanogenic Euryarchaeota produces predominantly GDGT-0 (Schouten et al., 2013). It has been proposed that the GDGT-0/Cren and MI ratios can be used to infer the relative contribution of GDGTs from methanogenic Euryarchaeota *vs*

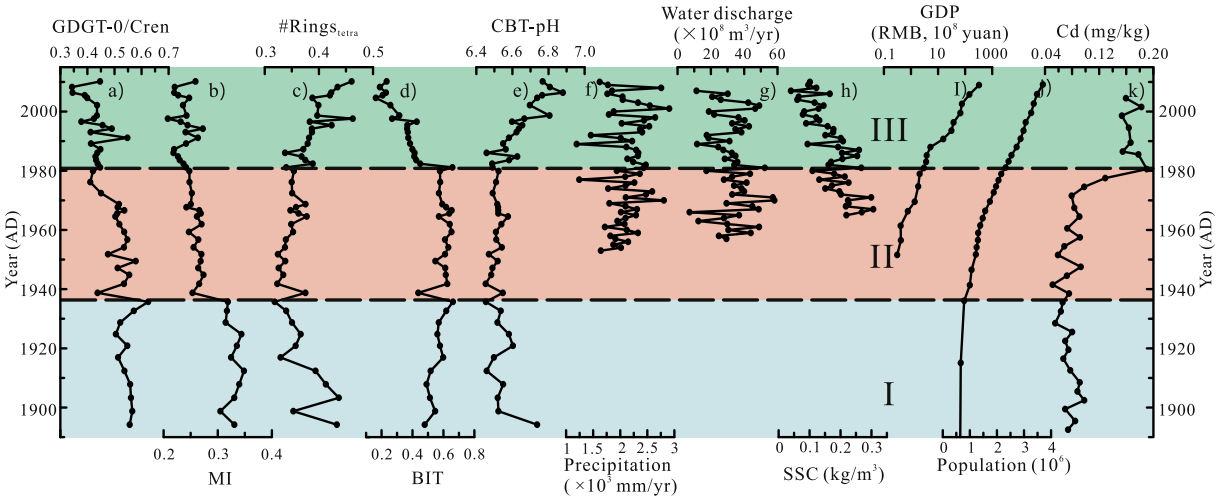

Fig. 4. Temporal variations of a) GDGT-0/Crenarchaeol ratios, b) MI ratios, c) #rings$_{tetra}$, d) BIT and e) CBT-pH in sediment core SN2. f) average annual precipitation at the Qinzhou Station (Ou and Zhao, 2017); g) annual water discharge from Qin River (Dai et al., 2011); h) annual Suspended Sediment Concentration (SSC) variation in the Nanliu River (Li et al., 2017); i) population of Qinzhou city (cited from www.gxdqw.com), j) industrial and agricultural production value (China Marine Statistical Yearbook, 1993) and (k) Cd content (Xia et al., 2012) are shown for comparison.

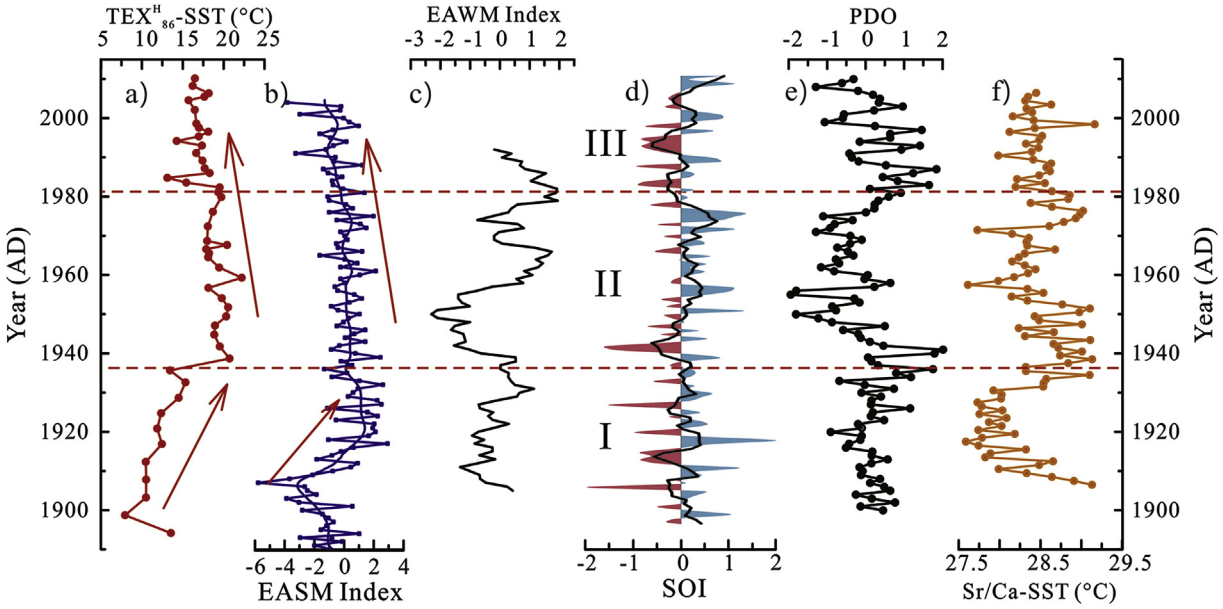

Fig. 5. Temporal variations of a) TEX$^{H}_{86}$-SST, b) Index of the East Asian Summer Monsoon (IPCC, 2013), c) Index of the East Asian Winter Monsoon (Zhou et al., 2007), d) Southern Oscillation Index (data from https://www.ncdc.noaa.gov/teleconnections/enso/indicators/soi/), e) the Pacific Decadal Oscillation index (Wooster and Zhang, 2004; http://research.jisao.washington.edu/pdo/PDO.latest) and f) Sr/Ca-SST of a Porites Coral from the Mischief Reef in the SCS (Lin et al., 2016). Solid lines in b) and d) are 5-yr running averages. Red and blue shadow in d) represents the El Niño and La Niña events, respectively. Green shadows represents the long-lasting and strong El Niño/La Niña events. (For interpretation of the references to colour in this figure legend, the reader is referred to the Web version of this article.)

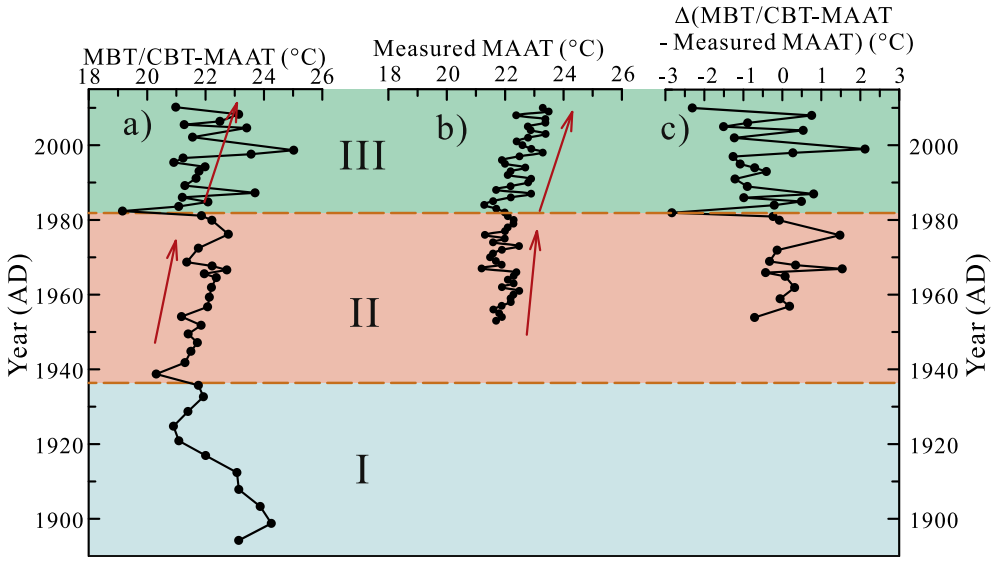

Fig. 6. a) MBT/CBT-MAAT in sediment core SN2 and its relationship with b) measured MAAT at Qinzhou Station (Ou and Zhao, 2017). The temporal discrepancy of GDGTs-based proxy and measured MAAT are shown in c) Δ (MBT/CBT-MAAT - measured MAAT).

Thaumarchaeota (Sinninghe Damsté et al., 2009; Xing et al., 2015). GDGT-0/Cren > 2 indicates a substantial methanogenic origin of GDGT-0 in lake (Blaga et al., 2009), while MI ratio higher than 0.3 in marine settings indicates the methanotrophic contribution of GDGT-0 (Zhang et al., 2011). The GDGT-0/Cren ratios in our dataset range from 0.34 to 0.62, and the MI range from 0.21 to 0.35 (Fig. 4a&b), suggesting an insignificant contribution of GDGTs from methanogenic and methanotrophic microbes. In addition, the concentrations of all the isoGDGTs were strongly correlated with that of crenarchaeol (Fig. 7), indicating that all the isoGDGTs are derived from a similar origin, namely Thaumarchaeota.

4.1.2. *BrGDGTs*

The brGDGTs occur ubiquitously in soils and peat worldwide (Weijers et al., 2006a), and thus represent terrestrial OM input to marine systems (Fietz et al., 2011). BrGDGTs in marine sediments are derived mainly from the erosion of soils and are transported through rivers to the coastal marine environment (Weijers et al., 2007a, 2007b). As the surface soils are often weak acidic in the Guangxi Province (Yang et al., 2014), the brGDGTs are dominated by acyclic brGDGTs. At the same time, the relatively high air temperatures lead to a low degree of methylation of brGDGTs, resulting in an overall dominance of GDGT-Ia in the core sediments. However, *in situ* production of branched GDGTs in aquatic environment was observed (Zhu et al., 2011; Hu et al., 2012; Weijers et al., 2014; Zhou et al., 2014), raising the complication of

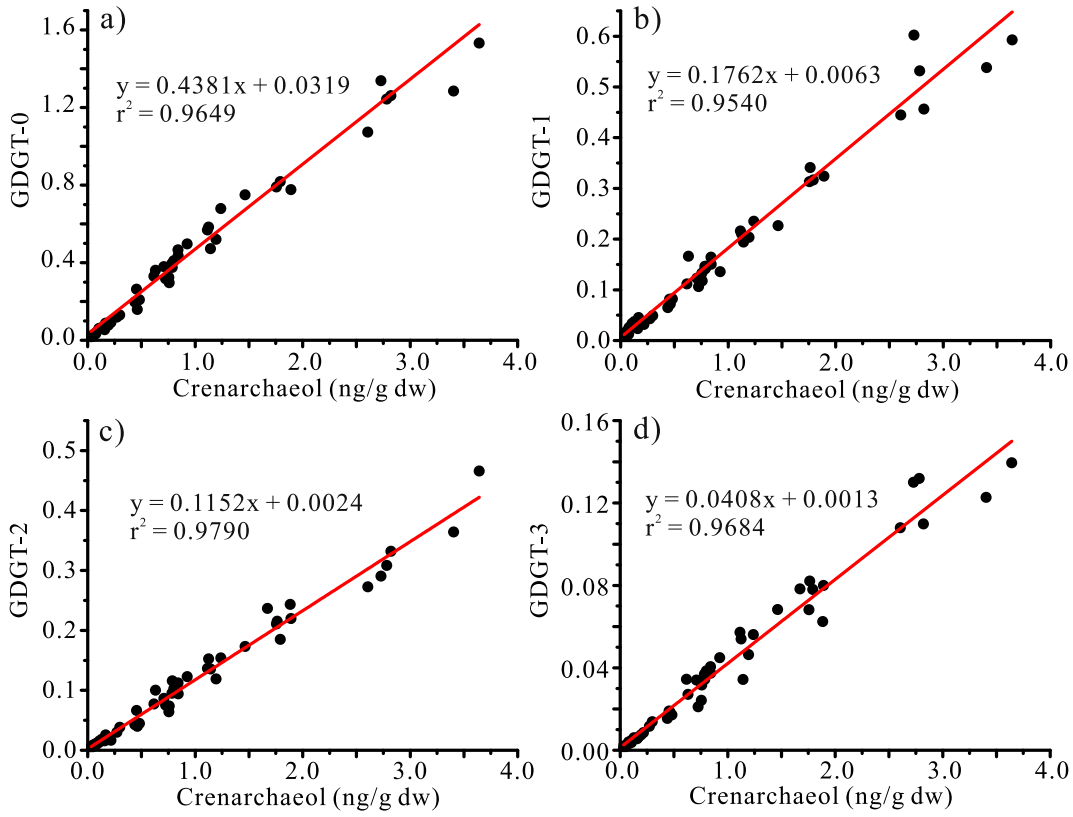

Fig. 7. Cross-plots between concentrations of crenarchaeol and a) GDGT-0, b) GDGT-1, c) GDGT-2 and d) GDGT-3 in sediments from Core SN2.

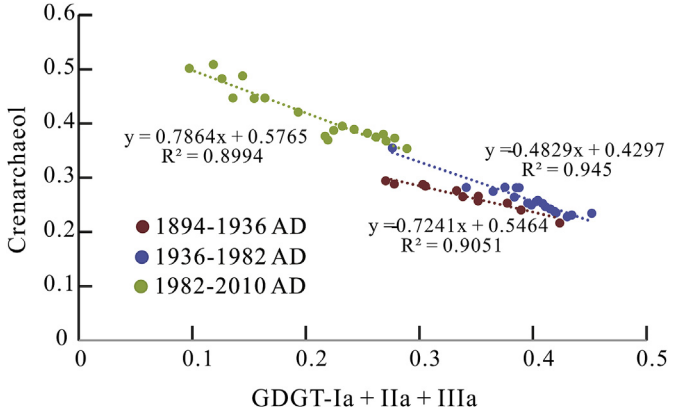

Fig. 8. Correlation between fractional abundance of major brGDGTs and Crenarchaeol. Sediments from Section I, II, III in core SN2 are shown in red, blue and green, respectively. (For interpretation of the references to colour in this figure legend, the reader is referred to the Web version of this article.)

origin of brGDGTs. Sinninghe Damsté (2016) proposed the #rings$_{tetra}$ value to distinguish soil-derived brGDGTs and *in situ* produced brGDGTs. In our core sediments, the #rings$_{tetra}$ values are all smaller than 0.7 (Fig. 4c), indicating that the brGDGTs are not mainly derived from marine *in situ* production. Meanwhile, as soil-derived brGDGTs are more strongly adsorbed onto terrestrial particles than the riverine *in situ* produced brGDGTs (Sinninghe Damsté, 2016), the *in situ* produced brGDGTs in rivers are extensively degraded (concentration decrease of ca. 95%) (Zhu et al., 2011). Thus, the riverine *in situ* produced brGDGTs should be of minor importance in the Beibu Gulf compared with the large tropical river systems, such as the Amazon and Berau rivers (Sinninghe Damsté, 2016). Previous study has demonstrated that the brGDGTs in surface sediments from the Sanniang Bay are mainly derived from soil erosion and transported to the location by rivers (Liao et al., 2018). The composition of brGDGTs in the Maowei Sea is similar to that in the outer Qinzhou Bay and Sanniang Bay, indicating that the brGDGTs are derived from the same source(s) in the Beibu Gulf (Liao et al., 2018).

The branched/isoprenoid tetraether (BIT) index is based on the relative abundance of soil derived tetraether lipids versus crenarchaeol, is capable of estimating the relative amounts of soil and aquatic OM in coastal marine, open ocean, and lake sediments (Hopmans et al., 2004). The BIT index ranges from 0.16 to 0.66 (Fig. 4d), with average of 0.49, suggesting that soil OM contribute significantly to the sediment core.

However, the #rings$_{tetra}$ index increased from average 0.35 to 0.40 from 1936–1982 AD to 1982–2010 AD (Fig. 4c), which indicate that the *in situ* production of brGDGTs increased (Sinninghe Damsté, 2016). At the same time, the CBT-pH decreased from section II to III (Fig. 4e), while the precipitation remained relatively constant (Fig. 4f, Ou and Zhao, 2017), suggesting that the change of CBT-pH was not caused by the variation of precipitation. Given that *in situ* production brGDGTs have a greater degree of cyclization, the change of CBT-pH might also be caused by the change of brGDGTs sources. Moreover, the correlation between brGDGT and Crenarchaeol change significantly from 1936–1982 AD to 1982–2010 AD (Fig. 8). The correlation coefficient (R^2) between fraction abundance of brGDGTs and Crenarchaeol decrease from 0.94 to 0.90. In our sediment core, it seems the Qinzhou River is the main source of brGDGTs and #rings$_{tetra}$ index showed that brGDGTs are mainly soil origin. Fietz et al., (2012) proposed three explanation for the good correlation of brGDGTs and crenarchaeol: physical processes in different source environment, common source environment of both GDGT types and mixed origins. Since the sources of isoGDGTs and brGDGTs have been assign to different species, the correlation between them might be caused by the fertilization effect (Fietz et al., 2012), which means the increase of Thaumarchaeota abundance might be caused by the increase of terrestrial nutrient input indicated by the brGDGTs. The decrease of R^2 indicates the scatter increase since 1982, which may be caused by the influence of other kind

of brGDGT—— *in situ* brGDGTs. Therefore, the proportion of *in situ* brGDGTs in the brGDGTs might be increasing after 1982 AD.

4.2. Reconstruction of temperatures

4.2.1. TEX_{86}^{H} temperature record

It has been proposed that the TEX_{86} proxy is only applicable to the reconstruction of SST if the isoGDGTs are derived from Thaumarchaeota and the BIT index is < 0.3 (Huguet et al., 2007; Weijers et al., 2006b; Zhu et al., 2011). In Core SN2, the BIT indices are generally > 0.3. However, as discussed above, the isoGDGTs were indeed derived predominantly from Thaumarchaeota. Moreover, there is no apparent correlation between TEX_{86} and BIT index (r^2 = 0.01) in our samples. Thus, it seems that the TEX_{86}^{H} temperature record is nearly not affected by terrestrial input (Huguet et al., 2007).

However, the TEX_{86}^{H}-derived SST (7.9–22.2 °C, Fig. 5a) are generally lower than the annual mean SST (23.9 °C) at the Qinzhou Station. Since the water depth of the Sanniang Bay is lower than 10 m, the temperature of surface water and subsurface water are almost the same, which rule out the subsurface production of Thaumarchaeota. Thus the low TEX_{86}^{H}-derived values in the record might be mainly due to the fact that Thaumarchaeota thrive primarily during colder seasons in the northern SCS (Jia et al., 2017; Wei et al., 2011; Ge et al., 2013; Zhang et al., 2013). The TEX_{86}^{H}-derived SST values of surface sediments are generally lower than the annual mean SST in the coastal northern SCS, indicating that the seasonal production of isoGDGTs may be bias toward winter (Strong et al., 2012; Zhou et al., 2014). Moreover, the TEX_{86}^{H}-derived SST in the surface sediment of the Qinzhou Bay and the Sanniang Bay are ranged from 14.8 to 21.6 °C, which are also lower than the annual mean SST (Liao et al., 2018). The TEX_{86}^{H}-derived SST values of core-top sediments of SN2 is 16.5 °C, which is consistent with the TEXH 86-derived SST values of surface sediment in the Qinzhou Bay and the Sanniang Bay. Also, the TEX_{86}^{H}-derived SST value of our core-top sediment is comparable to the winter SST of Qinzhou Bay, which is 15.2 °C (Chen et al., 1994).

In Core SN2, the TEX_{86}^{H}-derived SST increased from 7.9 °C in 1899 AD to 15.3 °C in 1936 AD, remained relatively stable at ~19.3 °C throughout 1936–1982 AD and decreased slowly from 19.3 °C to 16.5 °C after 1982 AD (Fig. 5a). As there is no long term *in situ* water temperature record available in the Qinzhou Bay, the TEX_{86}^{H}-derived SST record in SN2 were compared with the climate factors in order to figure out the controlling on the variation of SST and see if it is reflecting the natural variation. The strength of the East Asian Summer Monsoon (EASM), which indicated by the EASM Index (Wang et al., 2008), decreased from 1890 AD to 1910 AD and then increased to the strongest at 1920 AD. After 1920, it decreased gradually towards 2010 (Fig. 5b). The decreasing of TEX_{86}^{H}-derived SST from 1940 AD may be caused by the weakening of EASM. As EASM intensity weaken, the flow of warm and humid air from the ocean decreases, which would result in an decrease in SSTs by heat transfer through the air to sea water. However, the TEX_{86}^{H}-derived SST remained relatively low from 1920 AD to 1935 AD, while the EASM intensity has already increased at this period. In this period, the East Asia Winter Monsoon (EAWM) was at the strongest period since 1890, as indicated by the EAWM index (Fig. 5c, Zhou et al., 2007). Meanwhile, the coral records in the South China Sea also indicated that the EAWM was strongest during this period (Jiang et al., 2018; Song et al., 2012). The winter temperature was relatively low due to the strong north wind brought by the EAWM. Thus, the SST remained relatively low during this time.

Except for the monsoons, the El Niño-Southern Oscillation (ENSO) and the Pacific Decadal Oscillation (PDO) events have their own way to impact the TEX_{86}^{H}-derived SST. The ENSO intensity can be represented by the Southern Oscillation Index (SOI) and the PDO intensity can be represented by PDO index. Since the ENSO intensity is generally negatively correlated with PDO intensity (Kwon et al., 2013), their impact can be discussed together. In 1894–1936 AD, the SOI values were relatively low, indicating the El Niño events were stronger in this period (Fig. 5d&e). In 1936–1982 AD, the SOI values increased, indicating the La Niña events were more common (Fig. 5d&e). In 1982–2010 AD, the PDO indices were relatively high and the SOI values showed no obvious trend (Fig. 5d&e). The ENSO events influence the SST in the SCS through influencing the EAWM. The EAWM intensifies during the La Niña years, cooling the sea surface water, and weakens during the El Niño years, warming the sea surface water (Jhun and Lee, 2004; Wang et al., 2000). The temporal trend in the TEX_{86}^{H}-derived SST record was different from that of the PDO and SOI, suggesting that these events are not the primary factors that impacts the SSTs. However, the long-lasting and strong El Niño/La Niña events might be related to the increase/decrease of TEX_{86}^{H}-derived SST values (Fig. 5d). The slightly increase of TEX_{86}^{H}-derived SST might be influenced by the strong El Niño events, while the slightly decrease of TEX_{86}^{H}-derived SST might be influenced by La Niña events. The warming in El Niño years and the cooling in La Niña years are also recorded in the meteorological record at the Qinzhou Station (Li et al., 2000). Therefore, the ENSO events have a minor impact on the TEX_{86}^{H}-derived SST.

The temporal variation of TEX_{86}^{H}-derived SST record is compared to the SST record reconstructed by high-resolution Sr/Ca-SST of a Porites Coral from the Mischief Reef in the SCS (Lin et al., 2016). The Sr/Ca-SST values were relatively low during 1894–1936 AD, high in 1936–1982 AD and decreased toward 2010 AD, displaying a similar trend with the TEX_{86}^{H}-derived SST in our samples (Fig. 5f). Thus, it seems that the TEX_{86}^{H}-derived SST in Core SN2 is consistent with the reconstructed paleotemperatures by other proxies in this region.

4.2.2. MBT/CBT temperature record

By comparison, the brGDGTs in the sediments of the gulf are mainly derived from soil erosion and transported to the location by rivers (Liao et al., 2018). Therefore, the brGDGT-based MBT and CBT proxies can be used to reconstruct the air temperature of the river discharge area. The MBT/CBT-based MAAT is showed in Fig. 6a. The reconstructed MAAT decreased from 24.3 °C in 1894 AD to 21.8 °C in 1936 AD, increased slowly from 20.3 °C to 22.8 °C in 1936–1982 AD. After 1982 AD, the reconstructed MAAT varied largely with a slightly increasing trend. The temporal trend of reconstructed MAAT matches well with the measured MAAT during 1951–1982 (Fig. 6b, Ou and Zhao, 2017), and the average discrepancy is 0.45 °C (Fig. 6c). However, the reconstructed MAAT varied sharply after 1982 AD, even though the trend is still similar to the measured MAAT (Fig. 6c). The average discrepancy of them increases to 1.08 °C in this period. As discuss above, the *in situ* production of brGDGTs proportion increased after 1982 AD and they have a greater degree of cyclization, which might cause the scatter in the CBT value and the reconstructed MAAT. Throughout this period, the concentration of brGDGTs did not increase (Fig. 3a), but the $\#rings_{tetra}$ index indicate that the *in situ* production of brGDGTs increased (Fig. 4c). Therefore, the scatter in the reconstructed MAAT might be caused by the increased content of *in situ* brGDGTs. Since the reconstruction of MAAT may be misled by the slightly change of brGDGTs sources, we need to figure out the cause for that and it is the major issue discussed below.

4.3. The anthropogenic influences on the environment

The BIT index decreased rapidly from 1982 to 1984 AD and decreased gradually afterword (Fig. 4d). Since the BIT values indicate the relative contribution of terrestrial soil OM to the marine OM, the terrestrial OM input might decrease in this period. We suggest that the decrease of terrestrial soil OM input to the Beibu Gulf sediments since 1982 AD may be related to the decrease in both runoff and the sediment discharges of the Qin River during this period. Runoff discharge of a river is normally affected by several factors. The river discharge decreased slowly from 1982 to 2010 except for the flooded years (Fig. 4g,

Dai et al., 2011). Meanwhile, the suspended sediment concentration (SSC) of the nearby Nanliu River decreased gradually from 1980 (Fig. 4h, Li et al., 2017). For all the factors, the annual precipitation may be the most important factor. However, based on the observation data, the annual precipitation in Qinzhou Station remained relatively constant (Fig. 4f, Ou and Zhao, 2017). Therefore, the change in annual precipitation cannot be the cause of the decrease in runoff discharges from Qin River. We suggest that human activities may have played important roles in this process. Since the 1980's, the Beibu Gulf area is under major economic development, and large changes have happened to many aspects, such as the utilization of fresh water resources. Large amounts of river water have been used to irrigate farmland, where rice cultivation is widespread. Furthermore, the constructions of dams in order to control flood and generate electricity have increased largely since then. Almost all of the increased industrial and agricultural production use the water resources and lead to the reduction of the runoff discharge of rivers. Meanwhile, the rapid increase in population has a significant need for domestic water supply, which might have led to a decrease in the runoff discharge of Qin River. Qinzhou City, in the north of Maowei Sea, has a long inhabited history, with a population of ca. 600,000 at 150 yr before present (Fig. 4i; Country yearbook of Qinzhou, 1991). Population increase from 600,000 to 2,000,000 before 1982, but increase from 2,000,000 to almost 4,000,000 from 1982 to 2010 (Fig. 4j), which requires a huge amount of domestic water.

Even though the dam construction between 1980 to 1985 change the physical properties in the sediments and reduce the concentration of GDGTs. The concentrations of isoGDGTs increased significantly after 1985 AD, while the concentration of brGDGTs remained relatively low. The increase of isoGDGTs concentration indicates the thriving of Thaumarchaeota. Since the 1980's, the human activities changed the land use and nutrient status of marine environment. Since 1982, with the start of economic growth in China, the GDP values increased rapidly (Fig. 4i). The economic development cause significant influence on the marine environment. With the intensive use of phosphate fertilizers and the combustion of fossil fuels after ca. 1980 AD, Cd showed a moderate enrichment (maximum 3.5-fold) relative to local background levels (Fig. 4k; Xia et al., 2011, 2012). The nitrogen input increase from 1980 AD and the increased nitrogen came from river discharge (Xu et al., 2012). Since the Thaumarchaeota depend on nutrient input, especially nitrogen (Brochier-Armanet et al., 2008), the nutrient increase since 1980 AD may cause the thriving of Thaumarchaeota. All these evidences indicate that even though the terrestrial material input decreased since 1982, nutrient input to the Beibu Gulf increased rapidly caused by human activities. The increasing nutrient in the bay might induce the thriving of Thaumarchaeota.

In summary, increased human activities rather than natural reasons are the main reasons for the decrease in terrestrial OM input, which change the sources of brGDGTs and lead to the discrepancy in CBT/MBT reconstructed MAAT. However, the source of isoGDGTs remains unchanged, suggesting that the TEX^{H}_{86} can be used to reconstruct the SST in this area.

5. Conclusions

Iso- and br-GDGTs were detected in the core sediments taken from the Beibu Gulf. The GDGT-0/Crenarchaeol values and the MI index show that the isoGDGTs are mainly derived from Thaumarchaeota, and the TEX_{86} index could be applied to reconstruct the temporal SST variation there. The comparison with climate factors showed that the TEX^{H}_{86} -derived SST is controlled mainly by the East Asia Monsoon and influenced minor by the PDO and ENSO events.

The compositions of brGDGTs and the MBT/CBT values suggest that the brGDGTs are mainly from terrestrial soil via river discharge. Even though the MBT/CBT can be used to reconstruct the MAAT before 1982, its validity was obscured by the scatter of MBT/CBT proxies after 1982, which might be caused by the increase of *in situ* brGDGT production. The BIT index decreased rapidly after 1982, corresponding to the rapid increase of human activities. The decrease in terrestrial OM input and the increase of nutrient loading caused the change of brGDGTs sources and led to the discrepancy in CBT/MBT reconstructed MAAT. Therefore, human influences on the organic proxies should be constraint before applying these proxies in centennial climate reconstruction.

Declaration of competing interest

I am authorized on behalf of all the authors of this manuscript to confirm that no author has any conflict of interest to disclose, all authors have approved the version submitted for publication, the work in this manuscript is original and has not been published previously, and the manuscript is not under consideration by any other journal.

Acknowledgements

We thank Prof. Thijs van Kolfschoten and three anonymous reviewers for critical review of earlier drafts of the manuscript. This work was supported by the National Key Research and Development Program (2016YFA0601204), National Natural Science Foundation of China (Nos. 41576053 and 41876058), Earmarked Foundation of Laboratory of Marine Ecosystem and Biogeochemistry, SOA (LMEB201712).This is also contribution No. IS-2785 from GIGCAS.

Appendix A. Supplementary data

Supplementary data to this article can be found online at https://doi.org/10.1016/j.quaint.2019.12.004.

References

Abram, N.J., McGregor, H.V., Tierney, J.E., Evans, M.N., McKay, N.P., Kaufman, D.S., Consortium, P.k., 2016. Early onset of industrial-era warming across the oceans and continents. Nature 536, 411–418.

Brochier-Armanet, C., Boussau, B., Gribaldo, S., Forterre, P., 2008. Mesophilic crenarchaeota: proposal for a third archaeal phylum, the Thaumarchaeota. Nat. Rev. Microbiol. 6, 245–252.

Canuel, E.A., Cammer, S.S., McIntosh, H.A., Pondell, C.R., 2012. Climate change impacts on the organic carbon cycle at the land-ocean interface. Annu. Rev. Earth Planet Sci. 40, 685–711.

Chen, L., Liu, J., Xing, L., Krauss, K.W., Wang, J., Xu, G., Li, L., 2017. Historical changes in organic matter input to the muddy sediments along the Zhejiang-Fujian Coast, China over the past 160 years. Org. Geochem. 111, 13–25.

Chen, L., Liu, J., Wang, J., Xu, G., Li, F., He, X., Zhang, Y., Li, L., 2018. Sources and distribution of tetraether lipids in sediments from the Zhejiang-Fujian coastal mud area, China, over the past 160 years: implications for paleoclimate change. Org. Geochem. 121, 114–125.

Chen, Z., Wu, S., Xia, D., 1998. The Bay Chorography in China (14). Ocean Press, Beijing (in Chinese).

Chen, Z., Xu, S., Qiu, Y., Lin, Z., Jia, X., 2009. Modeling the effects of fishery management and marine protected areas on the Beibu Gulf using spatial ecosystem simulation. Fish. Res. 100, 222–229.

Cloern, J.E., 2001. Our evolving conceptual model of the coastal eutrophication problem. Mar. Ecol. Prog. Ser. 210, 223–253.

Dai, J., Zhang, X., Wang, D., Fang, R., Guo, c., Li, H., 2011. Distribution characteristics and change trend of rainfall and runoff in Beibu gulf. China Rural Water and Hydropower 2011, 1–6 (in Chinese with English abstract).

de la Torre, J.R., Walker, C.B., Ingalls, A.E., Könneke, M., Stahl, D.A., 2008. Cultivation of a thermophilic ammonia oxidizing archaeon synthesizing crenarchaeol. Environ. Microbiol. 10, 810–818.

De Rosa, M., Gambacorta, A., 1988. The lipids of Archaebateria. Prog. Lipid Res. 27, 153–175.

Diaz, R.J., Rosenberg, R., 2008. Spreading dead zones and consequences for marine ecosystems. Science 321, 926–929.

Eglinton, T.I., Eglinton, G., 2008. Molecular proxies for paleoclimatology. Earth Planet. Sci. Lett. 275, 1–16.

Fietz, S., Martínez-Garcia, A., Rueda, G., Peck, V.L., Huguet, C., Escala, M., Rosell-Melé, A., 2011. Crenarchaea and phytoplankton coupling in sedimentary archives: common trigger or metabolic dependence? Limnol. Oceanogr. 56, 1907–1916.

Fietz, S., Huguet, C., Bendle, J., Escala, M., Gallacher, C., Herfort, L., Jamieson, R., Martínez-Garcia, A., McClymont, E.L., Peck, V.L., Prahl, F.G., Rossi, S., Rueda, G., Sanson-Barrera, A., Rosell-Melé, A., 2012. Co-variation of crenarchaeol and branched GDGTs in globally-distributed marine and freshwater sedimentary archives. Glob.

Planet. Chang. 92–93, 275–285.
Ge, H., Zhang, C.L., Dang, H., Zhu, C., Jia, G., 2013. Distribution of tetraether lipids in surface sediments of the northern South China Sea: implications for TEX86 proxies. Geosci. Front. 4, 223–229.
Ge, H., Zhang, C.L., Li, J., Versteegh, G.J.M., Hu, B., Zhao, J., Dong, L., 2014. Tetraether lipids from the southern yellow sea of China: implications for the variability of East Asia winter monsoon in the holocene. Org. Geochem. 70, 10–19.
Hopmans, E.C., Weijers, J.W.H., Schefuß, E., Herfort, L., Sinninghe Damsté, J.S., Schouten, S., 2004. A novel proxy for terrestrial organic matter in sediments based on branched and isoprenoid tetraether lipids. Earth Planet. Sci. Lett. 224, 107–116.
Huguet, C., Smittenberg, R.H., Boer, W., Sinninghe Damsté, J.S., Schouten, S., 2007. Twentieth century proxy records of temperature and soil organic matter input in the Drammensfjord, southern Norway. Org. Geochem. 38, 1838–1849.
IPCC, 2013. Climate Change 2013: the Physical Science Basis. Contribution of Working Group I to the Fifth Assessment Report of the Intergovernmental Panel on Climate Change. Cambridge University Press, Cambridge, United Kingdom and New York, NY, USA.
Jansen, E., Overpeck, J., Briffa, K.R., Duplessy, J.C., Joos, F., Masson-Delmotte, V., Olago, D., Otto-Bliesner, B., Peltier, W.R., Rahmstorf, S., Ramesh, R., Raynaud, D., Rind, D., Solomina, O., Villalba, R., Zhang, D., 2007. Palaeoclimate. In: Solomon, S., Qin, D., Manning, M., Chen, Z., Marquis, M., Averyt, K.B., Tignor, M., Miller, H.L. (Eds.), Climate Change 2007: the Physical Science Basis. Contribution of Working Group I to the Fourth Assessment Report of the Intergovernmental Panel on Climate Change. Cambridge University Press, Cambridge, United Kingdom and New York, NY, USA.
Jhun, J.G., Lee, E.J., 2004. A new East Asian winter monsoon index and associated characteristics of the winter monsoon. J. Clim. 17, 711–726.
Jia, G., Wang, X., Guo, W., Dong, L., 2017. Seasonal distribution of archaeal lipids in surface water and its constraint on their sources and the TEX_{86} temperature proxy in sediments of the South China Sea. Journal of Geophysical Research-Biogeosciences 122, 592–606.
Jiang, W., Yu, K., Song, Y., Zhao, J.-x., Feng, Y.-x., Wang, Y., Xu, S., Han, T., 2018. Annual REE signal of East Asian winter monsoon in surface seawater in the northern South China sea: evidence from a century-long porites coral record. Paleoceanography and Paleoclimatology 33, 168–178.
Kim, J.-H., van der Meer, J., Schouten, S., Helmke, P., Willmott, V., Sangiorgi, F., Koç, N., Hopmans, E.C., Damsté, J.S.S., 2010. New indices and calibrations derived from the distribution of crenarchaeal isoprenoid tetraether lipids: implications for past sea surface temperature reconstructions. Geochem. Cosmochim. Acta 74, 4639–4654.
Koga, Y., Morii, H., 2007. Biosynthesis of ether-type polar lipids in archaea and evolutionary considerations. Microbiol. Mol. Biol. Rev. 71, 97–120.
Kwon, M., Yeh, S.-W., Park, Y.-G., Lee, Y.-K., 2013. Changes in the linear relationship of ENSO-PDO under the global warming. Int. J. Climatol. 33, 1121–1128.
Lai, J., Jiang, F., Ke, K., Xu, M., Lei, F., Chen, B., 2014. Nutrients distribution and trophic status assessment in the northern Beibu Gulf, China. Chin. J. Oceanol. Limnol. 32, 1128–1144.
Lammers, J.M., van Soelen, E.E., Donders, T.H., Wagner-Cremer, F., Sinninghe Damsté, J.S., Reichart, G.J., 2013. Natural environmental changes versus human impact in a Florida estuary (Rookery bay, USA). Estuar. Coasts 36, 149–157.
Li, S., Dai, Z., Mei, X., Huang, H., Wei, W., Gao, J., 2017. Dramatic variations in water discharge and sediment load from Nanliu River (China) to the Beibu Gulf during 1960s–2013. Quat. Int. 440, 12–23.
Li, X., Li, Y., Zhang, Y., 2000. Statistic analysis to the effect of ENSO cases on Guangxi 's climate. Journal of Guangxi Meteorology 21, 21–25 (in Chinese with English abstract).
Liao, W., Hu, J., Zhou, H., Hu, J., Peng, P.a., Deng, W., 2018. Sources and distribution of sedimentary organic matter in the Beibu Gulf, China: application of multiple proxies. Mar. Chem. 206, 74–83.
Lin, Z., Yu, K., Shi, Q., Chen, T., Tao, S., 2016. Sea surface temperature variations during the last 100 years recorded in a porites coral from the mischief reef of sansha city. Trop. Geogr. 36, 27–33 (in Chinese with English abstract).
Lotze, H.K., 2010. Historical reconstruction of human-induced changes in US estuaries. In: In: Gibson, R.N., Atkinson, R.J.A., Gordon, J.D.M. (Eds.), Oceanography and Marine Biology: an Annual Review, vol 48. pp. 267–338.
Ma, F., Wang, Y., Li, Y., Ye, C., Xu, Z., Zhang, F., 2010. The application of geostatistics in grain size trend analysis: a case study of eastern Beibu Gulf. J. Geogr. Sci. 20, 77–90.
Meng, X., Xia, P., Li, Z., Meng, D., 2016. Mangrove degradation and response to anthropogenic disturbance in the Maowei Sea (SW China) since 1926 AD: mangrove-derived OM and pollen. Org. Geochem. 98, 166–175.
Meyers, P.A., 1997. Organic geochemical proxies of paleoceanographic, paleolimnologic, and paleoclimatic processes. Org. Geochem. 27, 213–250.
Ou, Y., Zhao, J., 2017. Effects of ENSO events on climate in Beibu gulf area of Guangxi during 1951-2010. Journal of Catastrophology 32, 228–234 (in Chinese with English abstract).
Owen, R.B., Lee, R., 2004. Human impacts on organic matter sedimentation in a proximal shelf setting, Hong Kong. Cont. Shelf Res. 24, 583–602.
Pancost, R.D., Hopmans, E.C., Sinninghe Damsté, J.S., Party, M.S.S., 2001. Archaeal lipids in Mediterranean cold seeps: molecular proxies for anaerobic methane oxidation. Geochem. Cosmochim. Acta 65, 1611–1627.
Pearson, A., Huang, Z., Ingalls, A.E., Romanek, C.S., Wiegel, J., Freeman, K.H., Smittenberg, R.H., Zhang, C.L., 2004. Nonmarine crenarchaeol in Nevada hot springs. Appl. Environ. Microbiol. 70, 5229–5237.
Peterse, F., Kim, J.-H., Schouten, S., Kristensen, D.K., Koç, N., Sinninghe Damsté, J.S., 2009. Constraints on the application of the MBT/CBT palaeothermometer at high latitude environments (Svalbard, Norway). Org. Geochem. 40, 692–699.
Peterse, F., van der Meer, J., Schouten, S., Weijers, J.W.H., Fierer, N., Jackson, R.B., Kim, J.-H., Sinninghe Damsté, J.S., 2012. Revised calibration of the MBT-CBT paleotemperature proxy based on branched tetraether membrane lipids in surface soils. Geochem. Cosmochim. Acta 96, 215–229.
Powers, L.A., Werne, J.P., Johnson, T.C., Hopmans, E.C., Sinninghe Damsté, J.S., Schouten, S., 2004. Crenarchaeotal membrane lipids in lake sediments: a new paleotemperature proxy for continental paleoclimate reconstruction? Geology 32, 613–616.
Powers, L., Werne, J.P., Vanderwoude, A.J., Sinninghe Damsté, J.S., Hopmans, E.C., Schouten, S., 2010. Applicability and calibration of the TEX_{86} paleothermometer in lakes. Org. Geochem. 41, 404–413.
Schouten, S., Hopmans, E.C., Schefuss, E., Sinninghe Damsté, J.S., 2002. Distributional variations in marine crenarchaeotal membrane lipids: a new tool for reconstructing ancient sea water temperatures? Earth Planet. Sci. Lett. 204, 265–274.
Schouten, S., Huguet, C., Hopmans, E.C., Kienhuis, M.V.M., Sinninghe Damsté, J.S., 2007. Analytical methodology for TEX_{86} paleothermometry by high-performance liquid chromatography/atmospheric pressure chemical ionization-mass spectrometry. Anal. Chem. 79, 2940–2944.
Schouten, S., Hopmans, E.C., Sinninghe Damsté, J.S., 2013. The organic geochemistry of glycerol dialkyl glycerol tetraether lipids: a review. Org. Geochem. 54, 19–61.
Sinninghe Damsté, J.S., Hopmans, E.C., Pancost, R.D., Schouten, S., Geenevasen, J.A.J., 2000. Newly discovered non-isoprenoid glycerol dialkyl glycerol tetraether lipids in sediments. Chem. Commun. 1683–1684.
Sinninghe Damsté, J.S., Ossebaar, J., Abbas, B., Schouten, S., Verschuren, D., 2009. Fluxes and distribution of tetraether lipids in an equatorial African lake: constraints on the application of the TEX_{86} palaeothermometer and BIT index in lacustrine settings. Geochem. Cosmochim. Acta 73, 4232–4249.
Sinninghe Damsté, J.S., 2016. Spatial heterogeneity of sources of branched tetraethers in shelf systems: the geochemistry of tetraethers in the Berau River delta (Kalimantan, Indonesia). Geochem. Cosmochim. Acta 186, 13–31.
Song, S., Peng, Z., Zhou, W., Liu, W., Liu, Y., Chen, T., 2012. Variation of the winter monsoon in South China Sea over the past 183years: evidence from oxygen isotopes in coral. Glob. Planet. Chang. 98–99, 131–138.
Strong, D.J., Flecker, R., Valdes, P.J., Wilkinson, I.P., Rees, J.G., Zong, Y.Q., Lloyd, J.M., Garrett, E., Pancost, R.D., 2012. Organic matter distribution in the modern sediments of the Pearl River Estuary. Org. Geochem. 49, 68–82.
Wang, B., Wu, R.G., Fu, X.H., 2000. Pacific-East Asian teleconnection: how does ENSO affect East Asian climate? J. Clim. 13, 1517–1536.
Wang, B., Wu, Z., Li, J., Liu, J., Chang, C.-P., Ding, Y., Wu, G., 2008. How to measure the strength of the East Asian summer monsoon. J. Clim. 21, 4449–4463.
Wei, Y., Wang, J., Liu, J., Dong, L., Li, L., Wang, H., Wang, P., Zhao, M., Zhang, C.L., 2011. Spatial variations in archaeal lipids of surface water and core-top sediments in the South China sea and their implications for paleoclimate studies. Appl. Environ. Microbiol. 77, 7479–7489.
Weijers, J.W.H., Schouten, S., Hopmans, E.C., Geenevasen, J.A.J., David, O.R.P., Coleman, J.M., Pancost, R.D., Sinninghe Damsté, J.S., 2006a. Membrane lipids of mesophilic anaerobic bacteria thriving in peats have typical archaeal traits. Environ. Microbiol. 8, 648–657.
Weijers, J.W.H., Schouten, S., Spaargaren, O.C., Sinninghe Damsté, J.S., 2006b. Occurrence and distribution of tetraether membrane lipids in soils: implications for the use of the TEX_{86} proxy and the BIT index. Org. Geochem. 37, 1680–1693.
Weijers, J.W.H., Schefuss, E., Schouten, S., Sinninghe Damsté, J.S., 2007a. Coupled thermal and hydrological evolution of tropical Africa over the last deglaciation. Science 315, 1701–1704.
Weijers, J.W.H., Schouten, S., van den Donker, J.C., Hopmans, E.C., Sinninghe Damsté, J.S., 2007b. Environmental controls on bacterial tetraether membrane lipid distribution in soils. Geochem. Cosmochim. Acta 71, 703–713.
Wooster, W.S., Zhang, C.I., 2004. Regime shifts in the North Pacific: early indications of the 1976–1977 event. Prog. Oceanogr. 60, 183–200.
Wu, W., Zhao, L., Pei, Y., Ding, W., Yang, H., Xu, Y., 2013. Variability of tetraether lipids in Yellow River-dominated continental margin during the past eight decades: implications for organic matter sources and river channel shifts. Org. Geochem. 60, 33–39.
Xia, P., Meng, X., Yin, P., Cao, Z., Wang, X., 2011. Eighty-year sedimentary record of heavy metal inputs in the intertidal sediments from the Nanliu River estuary, Beibu Gulf of South China Sea. Environ. Pollut. 159, 92–99.
Xia, P., Meng, X., Feng, A., Yin, P., Wang, X., Zhang, J., 2012. 210Pb chronology and trace metal geochemistry in the intertidal sediment of Qinjiang River estuary, China. J. Ocean Univ. China 11, 165–173.
Xing, L., Sachs, J.P., Gao, W., Tao, S., Zhao, X., Li, L., Liu, Y., Zhao, M., 2015. TEX_{86} paleothermometer as an indication of bottom water temperature in the Yellow Sea. Org. Geochem. 86, 19–31.
Xu, M., Han, X., Long, Y., 2012. Analysis of the variation trend and sources of nitrogen and phosphorus in Qinzhou bay in the last 30 years. J. Environ. Eng. Technol. 2, 253–258 (in Chinese with English abstract).
Yang, H., Pancost, R.D., Dang, X., Zhou, X., Evershed, R.P., Xiao, G., Tang, C., Gao, L., Guo, Z., Xie, S., 2014. Correlations between microbial tetraether lipids and environmental variables in Chinese soils: optimizing the paleo-reconstructions in semi-arid and arid regions. Geochem. Cosmochim. Acta 126, 49–69.
Zell, C., Kim, J.H., Balsinha, M., Dorhout, D., Fernandes, C., Baas, M., Sinninghe Damsté, J.S., 2014. Transport of branched tetraether lipids from the Tagus River basin to the coastal ocean of the Portuguese margin: consequences for the interpretation of the MBT'/CBT paleothermometer. Biogeosciences 11, 5637–5655.
Zhang, J., Bai, Y., Xu, S., Lei, F., Jia, G., 2013. Alkenone and tetraether lipids reflect different seasonal seawater temperatures in the coastal northern South China Sea. Org. Geochem. 58, 115–120.
Zhang, J., Li, Y., Wang, Y., Zhang, Y., Zhang, D., Zhang, R., Li, J., Zhang, G., 2014. Spatial distribution and ecological risk of polychlorinated biphenyls in sediments from

Qinzhou Bay, Beibu Gulf of South China. Mar. Pollut. Bull. 80, 338–343.
Zhang, Y.G., Zhang, C.L., Liu, X.-L., Li, L., Hinrichs, K.-U., Noakes, J.E., 2011. Methane Index: a tetraether archaeal lipid biomarker indicator for detecting the instability of marine gas hydrates. Earth Planet. Sci. Lett. 307, 525–534.
Zheng, Q., Zhang, R., Wang, Y., Pan, X., Tang, J., Zhang, G., 2012. Occurrence and distribution of antibiotics in the Beibu Gulf, China: impacts of river discharge and aquaculture activities. Mar. Environ. Res. 78, 26–33.
Zhou, H., Hu, J., Spiro, B., Peng, P.a., Tang, J., 2014. Glycerol dialkyl glycerol tetraethers in surficial coastal and open marine sediments around China: indicators of sea surface temperature and effects of their sources. Palaeogeogr. Palaeoclimatol. Palaeoecol. 395, 114–121.
Zhou, W., Wang, X., Zhou, T.J., Li, C., Chan, J.C.L., 2007. Interdecadal variability of the relationship between the East Asian winter monsoon and ENSO. Meteorol. Atmos. Phys. 98, 283–293.
Zhu, C., Weijers, J.W.H., Wagner, T., Pan, J.M., Chen, J.F., Pancost, R.D., 2011. Sources and distributions of tetraether lipids in surface sediments across a large river-dominated continental margin. Org. Geochem. 42, 376–386.